asym_atl1

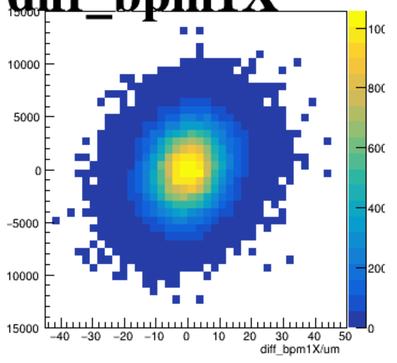

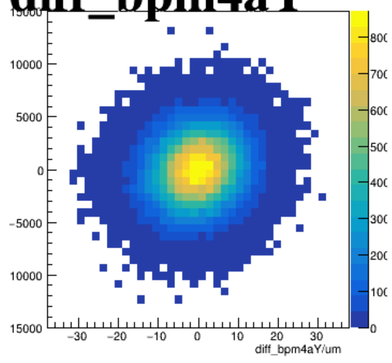

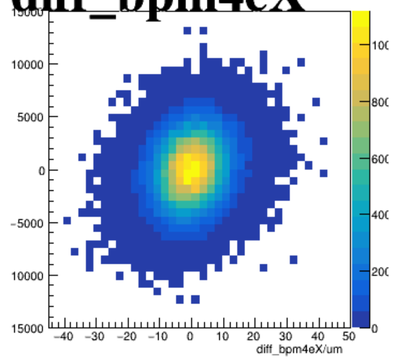

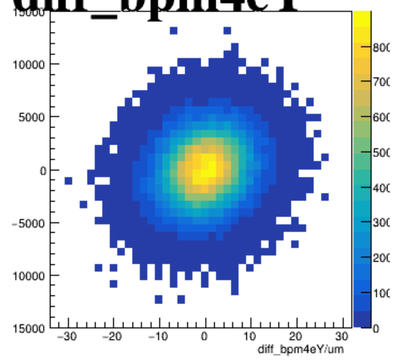

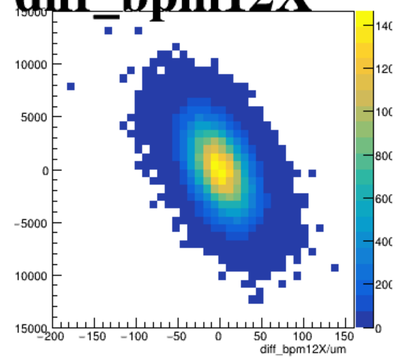

asym_atr1

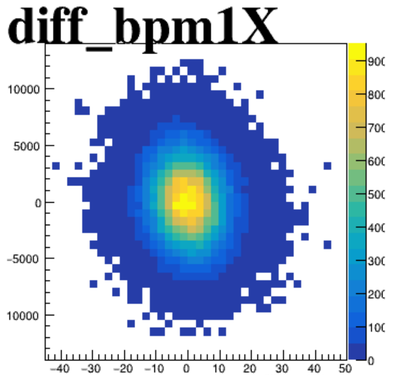

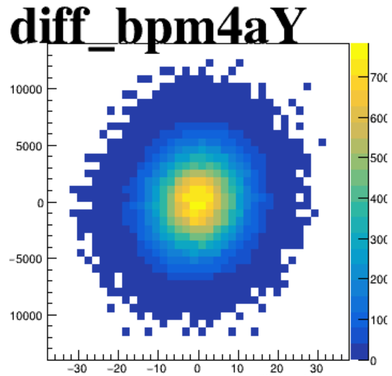

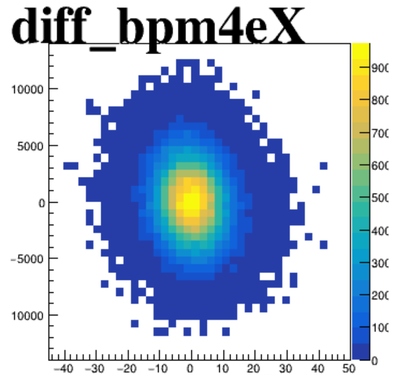

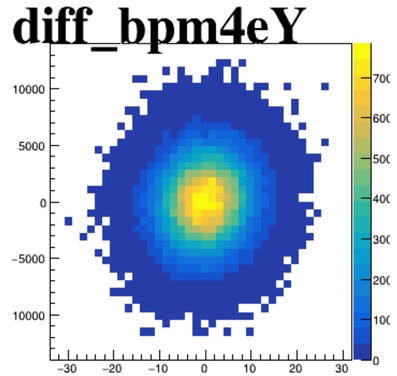

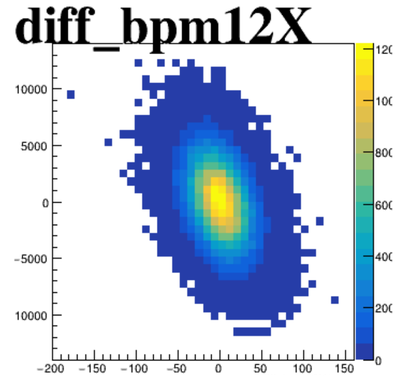

asym_atl2

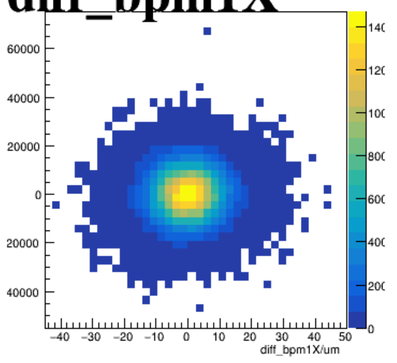

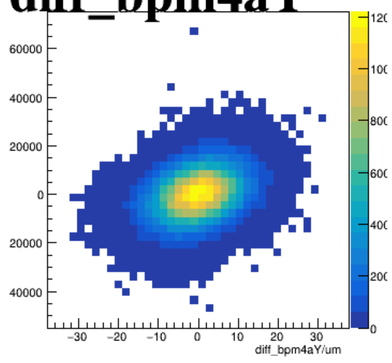

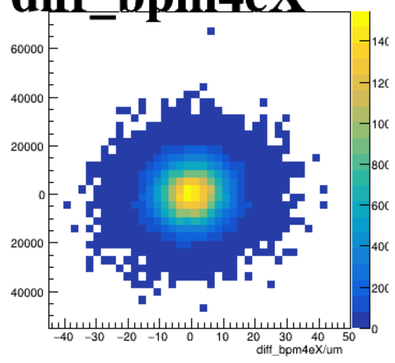

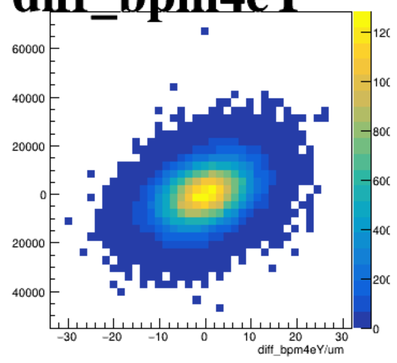

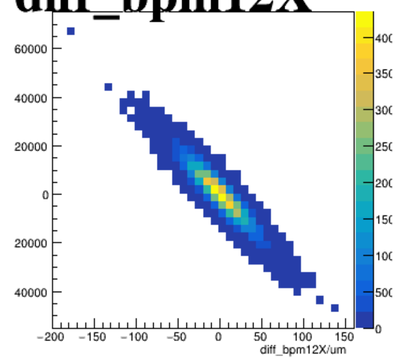

asym_atr2

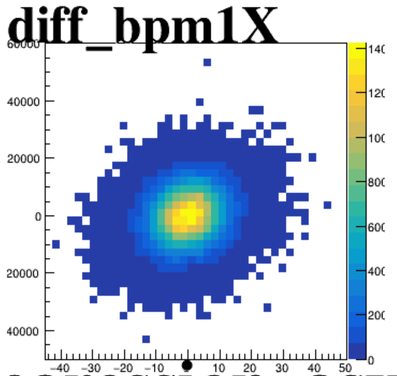

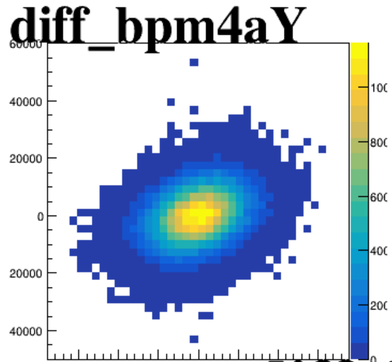

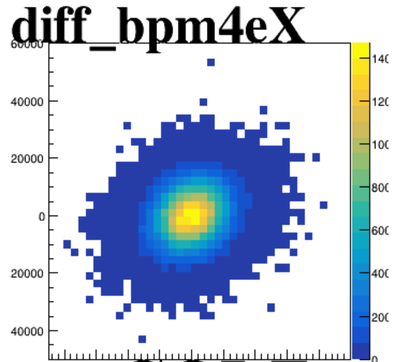

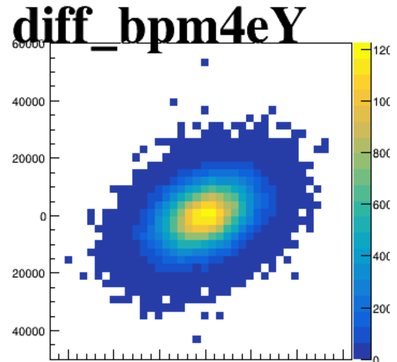

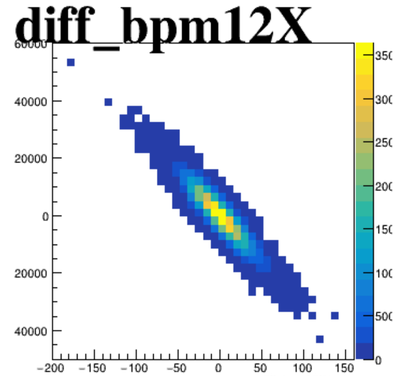

run6630_000_regression_asym_at_vs_diff_bpm-COLZ_postpan.png

reg_asym_atl1

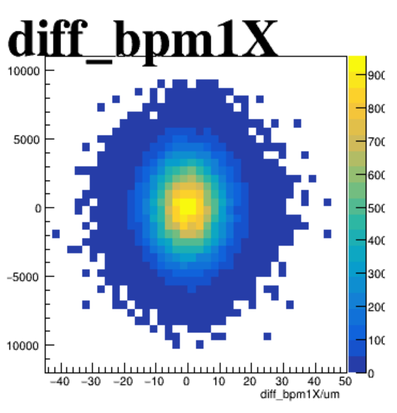

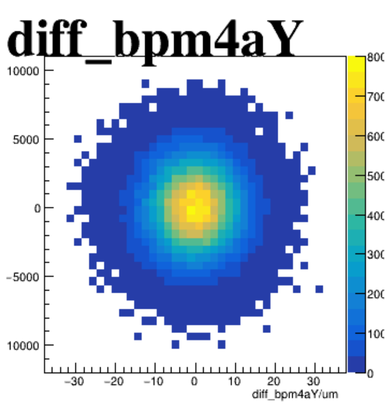

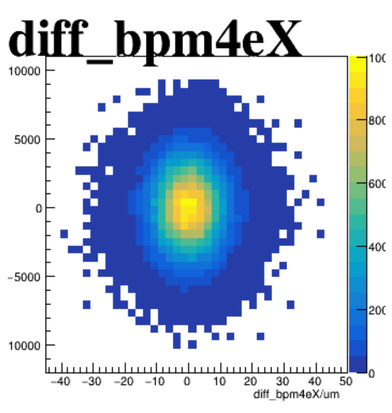

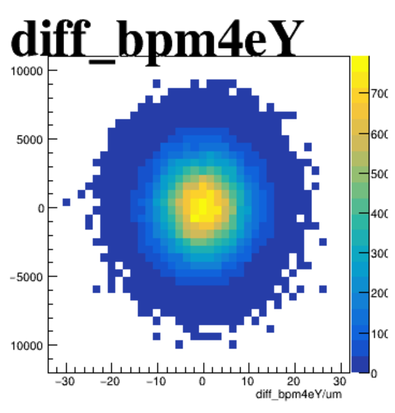

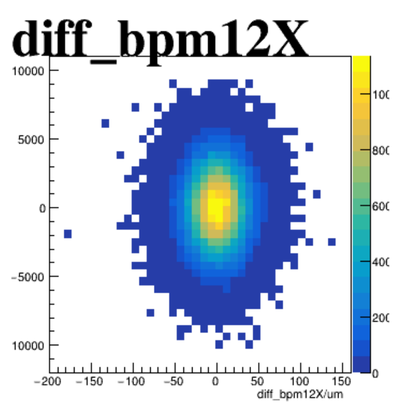

reg_asym_atr1

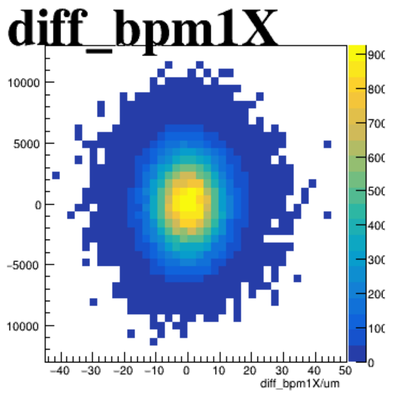

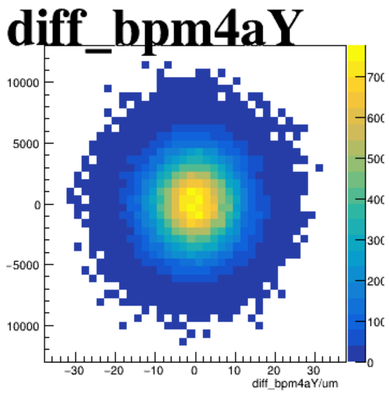

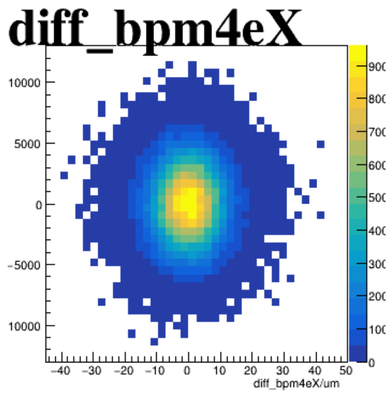

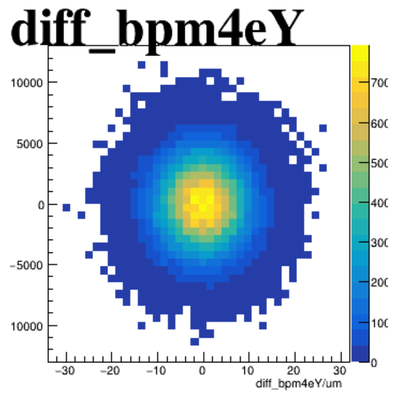

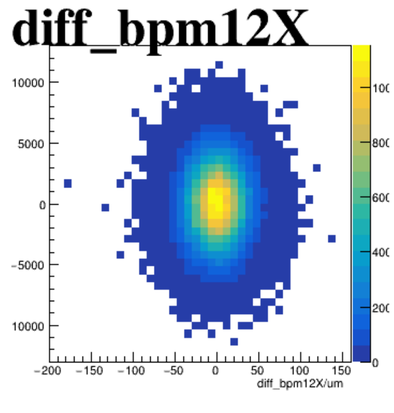

reg_asym_atl2

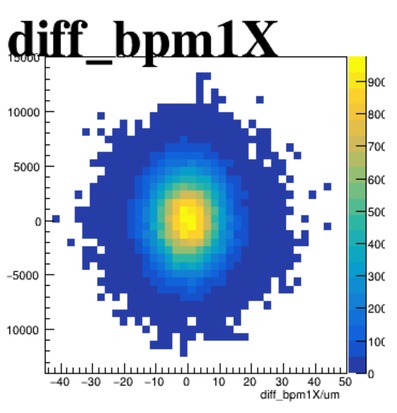

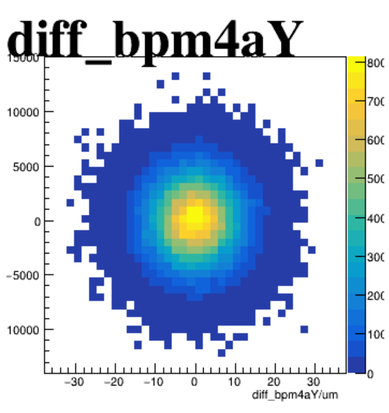

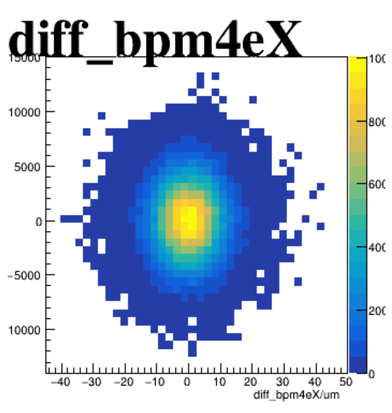

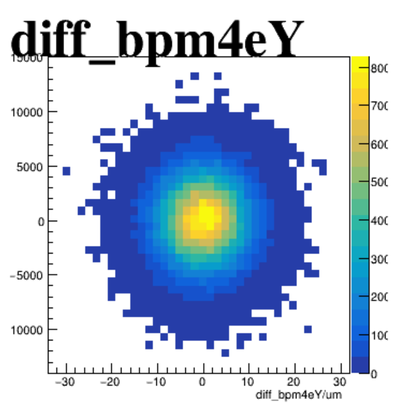

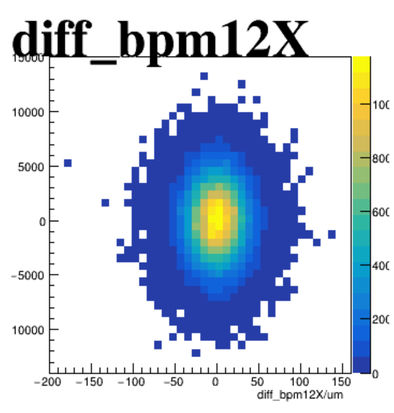

reg_asym_atr2

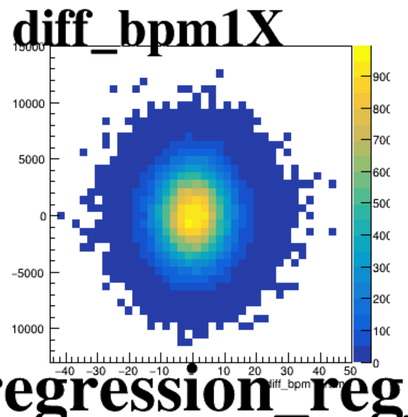

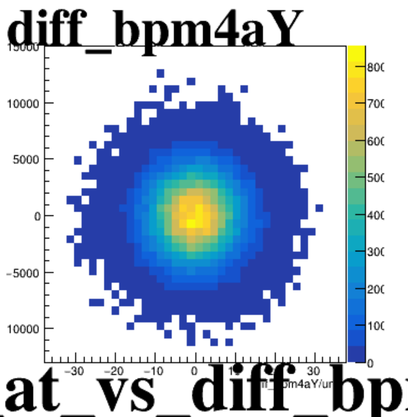

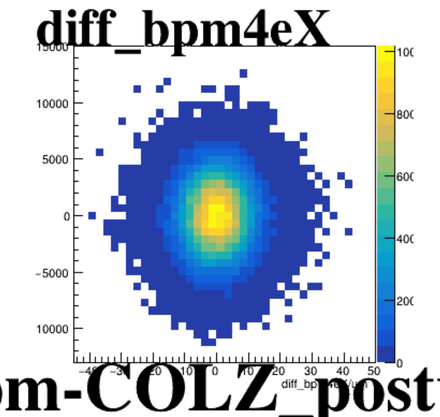

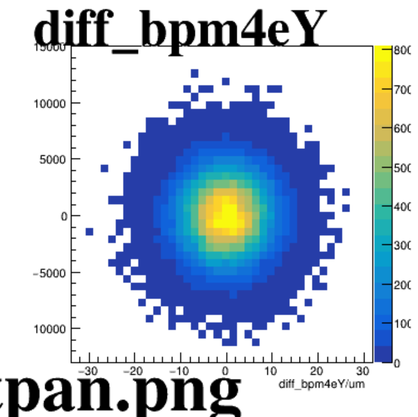

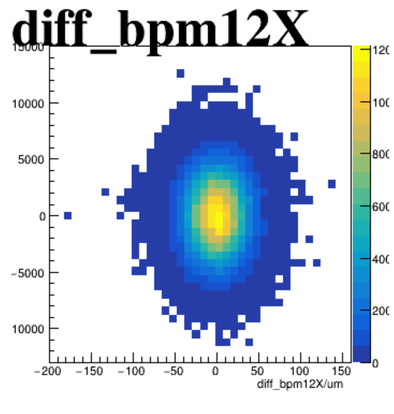

run6630_000_regression_reg_at_vs_diff_bpm-COLZ_postpan.png

asym_atl1

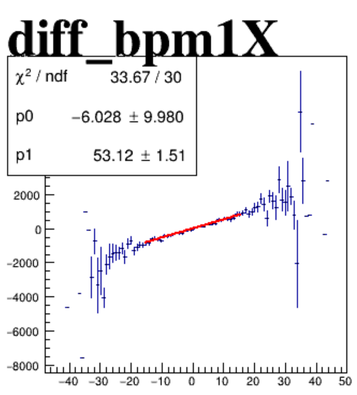

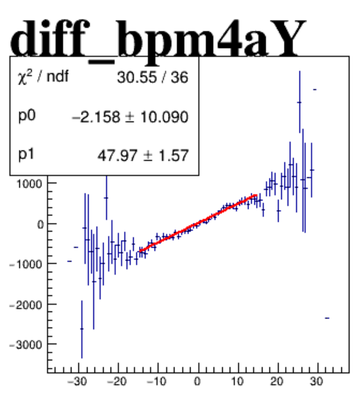

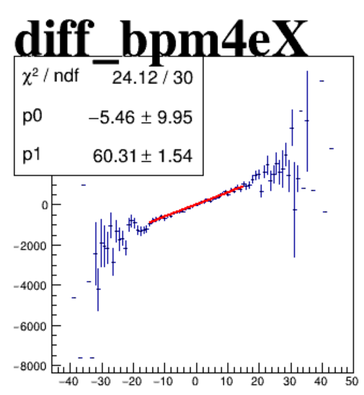

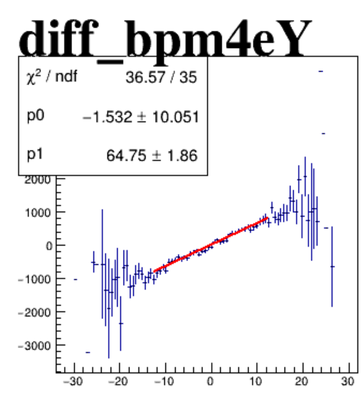

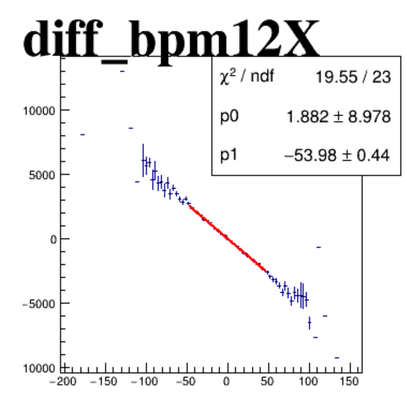

asym_atr1

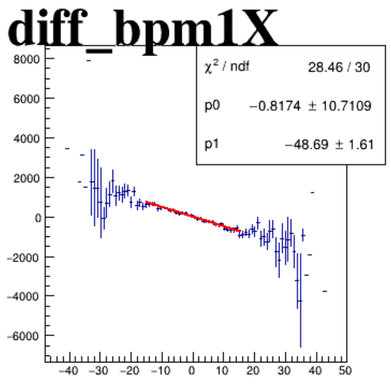

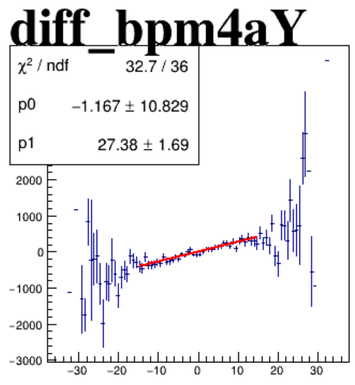

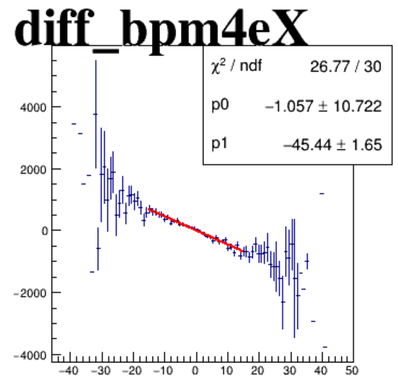

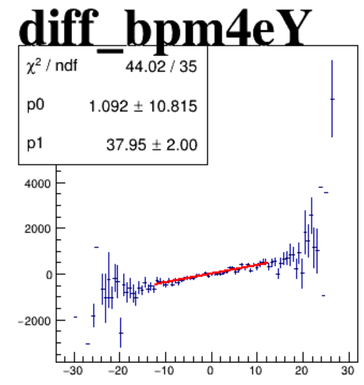

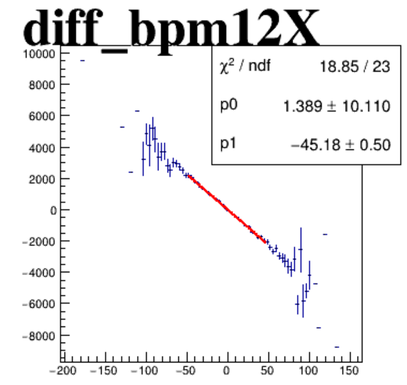

asym_atl2

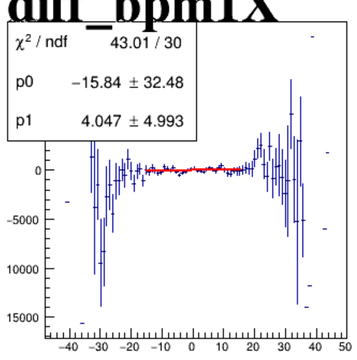

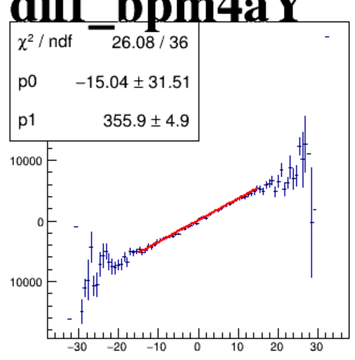

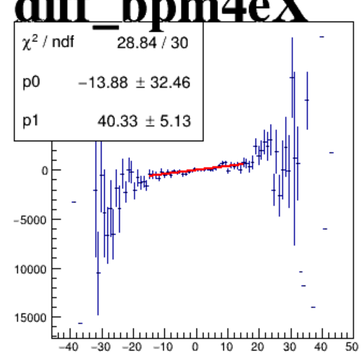

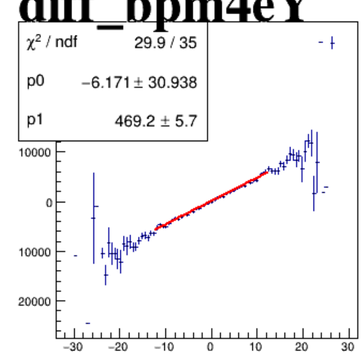

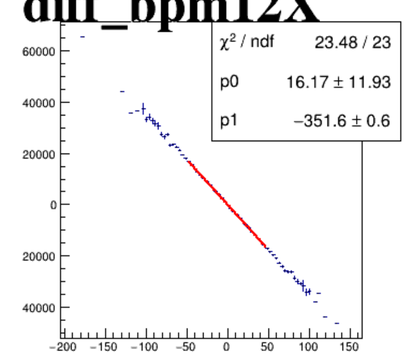

asym_atr2

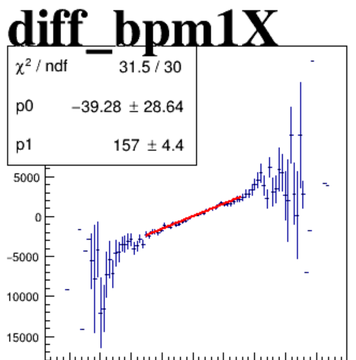

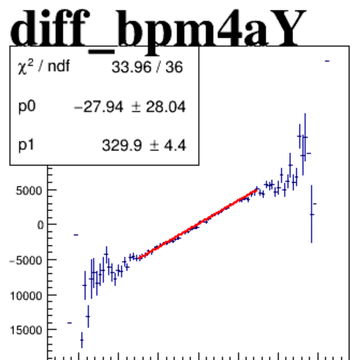

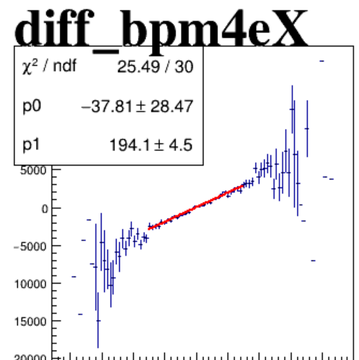

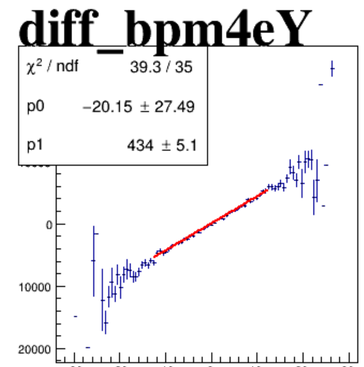

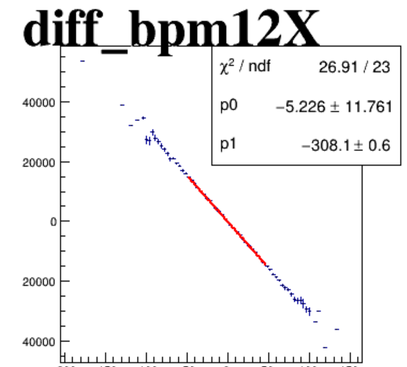

run6630_000_regression_asym_at_vs_diff_bpm-fit_postpan.png

reg_asym_atl1

diff_bpm1X

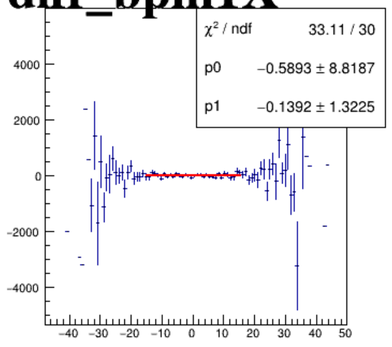

diff_bpm4aY

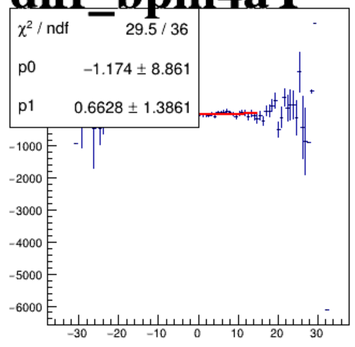

diff_bpm4eX

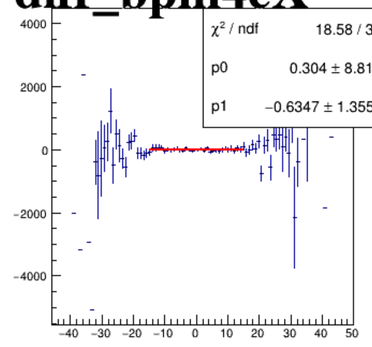

diff_bpm4eY

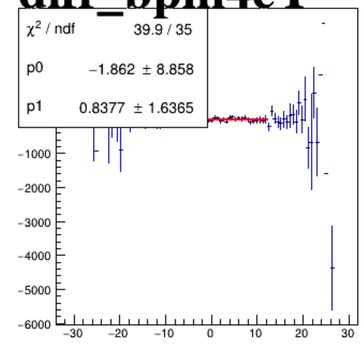

diff_bpm12X

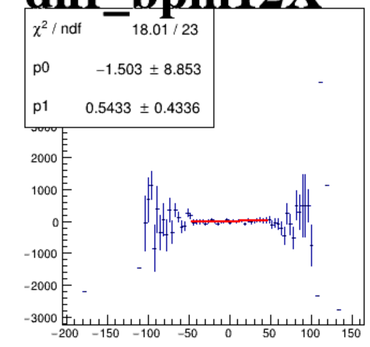

reg_asym_atr1

diff_bpm1X

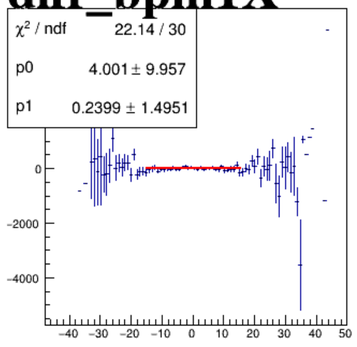

diff_bpm4aY

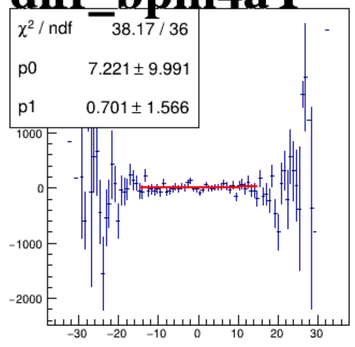

diff_bpm4eX

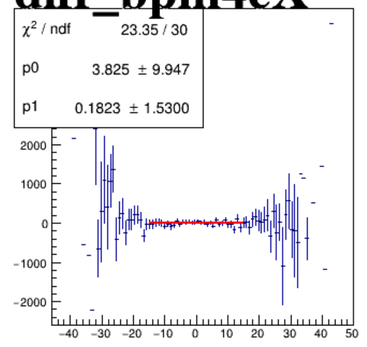

diff_bpm4eY

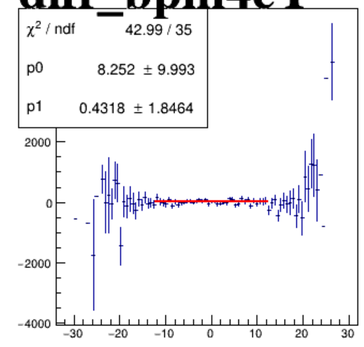

diff_bpm12X

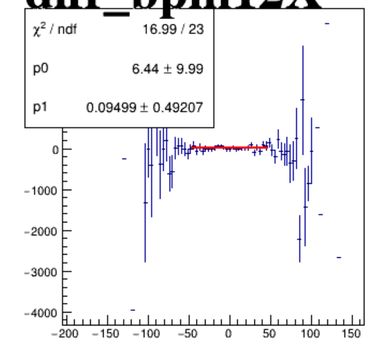

reg_asym_atl2

diff_bpm1X

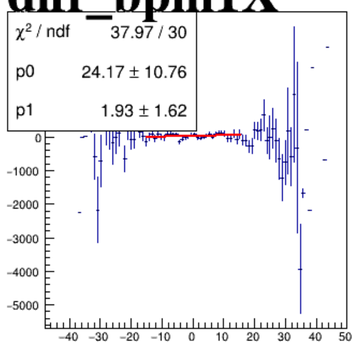

diff_bpm4aY

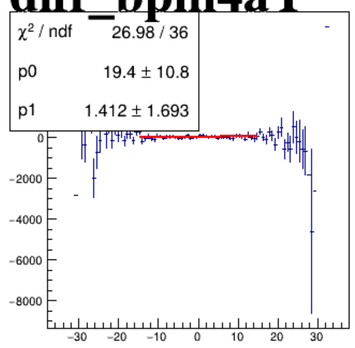

diff_bpm4eX

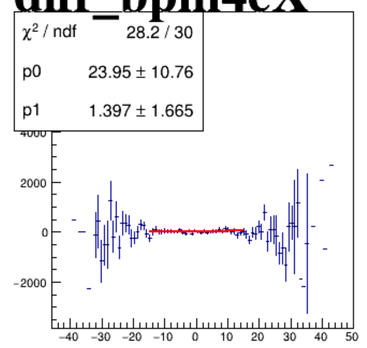

diff_bpm4eY

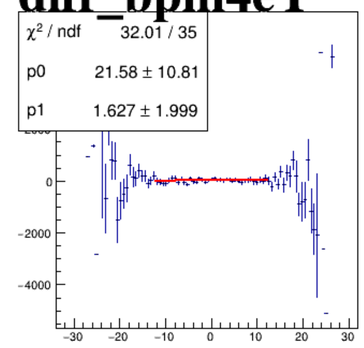

diff_bpm12X

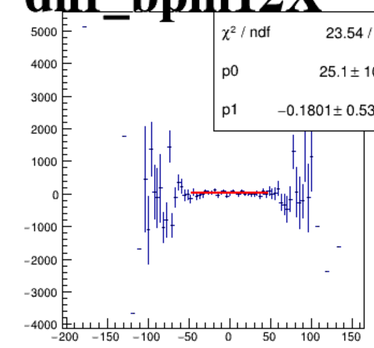

reg_asym_atr2

diff_bpm1X

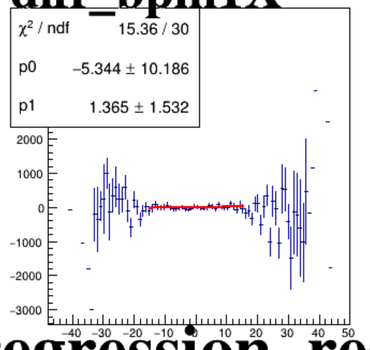

diff_bpm4aY

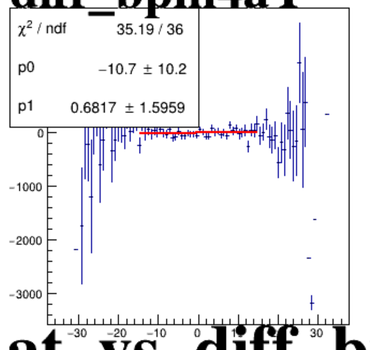

diff_bpm4eX

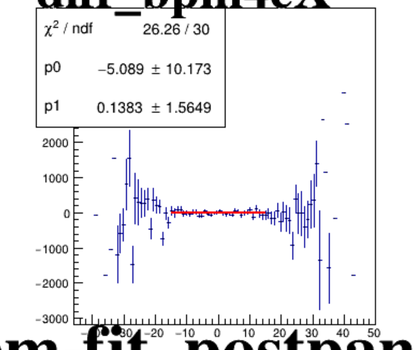

diff_bpm4eY

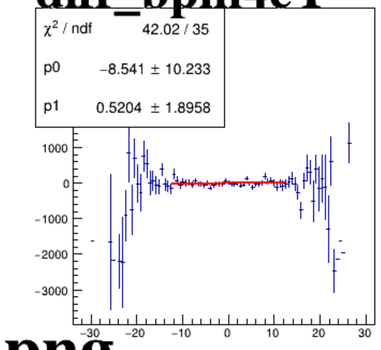

diff_bpm12X

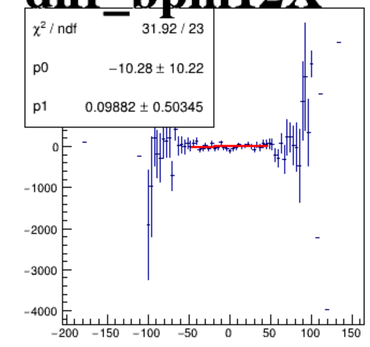

run6630_000_regression_reg_at_vs_diff_bpm-fit_postpan.png

asym_atl1

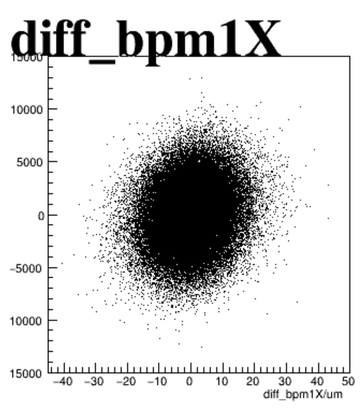

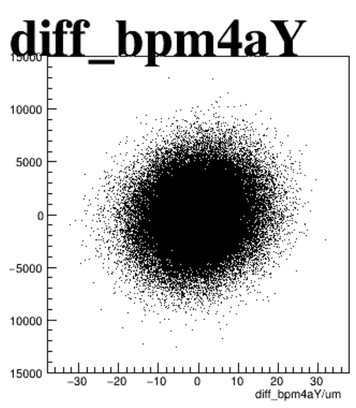

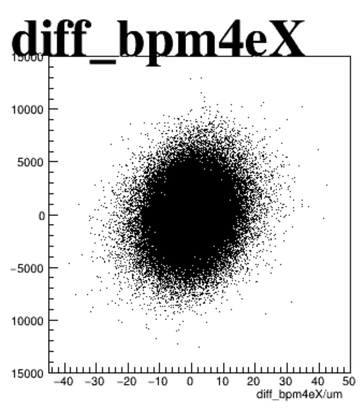

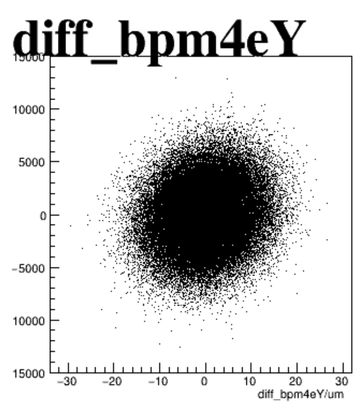

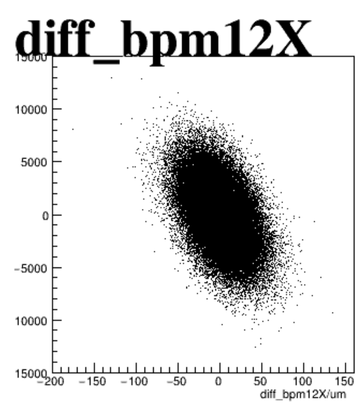

asym_atr1

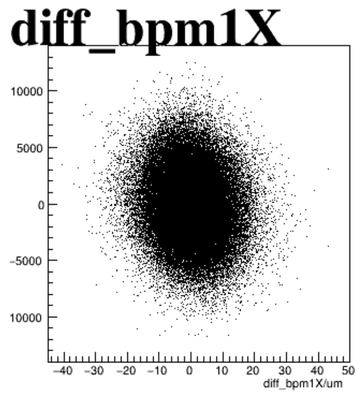

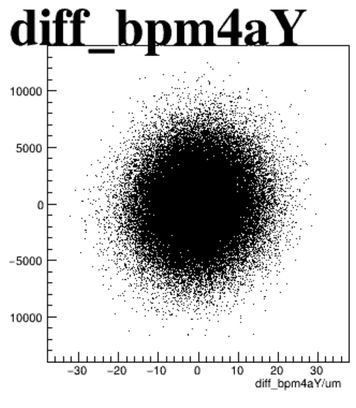

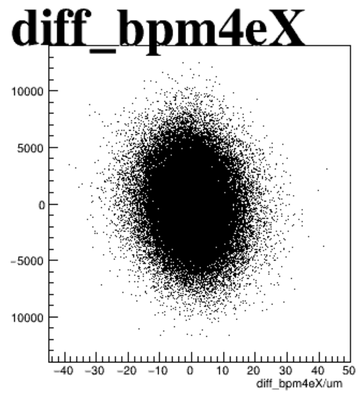

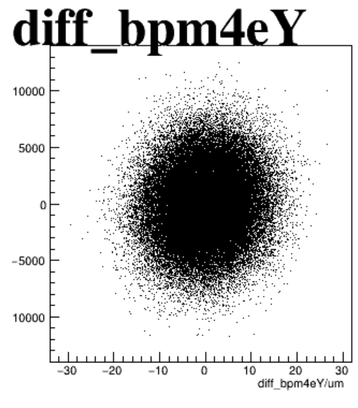

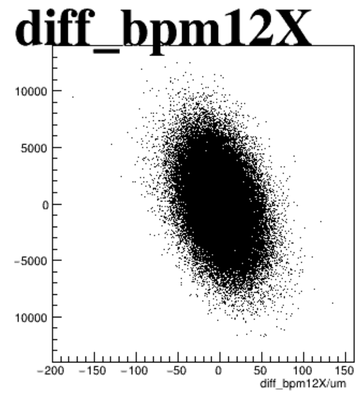

asym_atl2

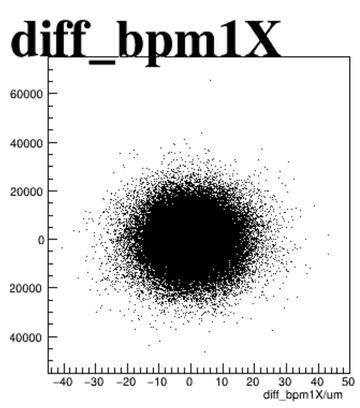

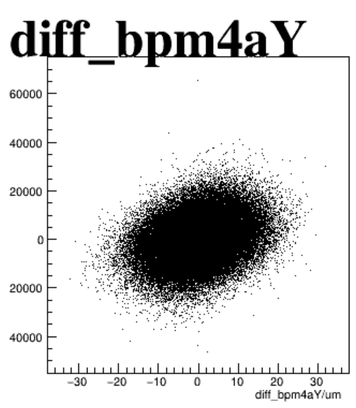

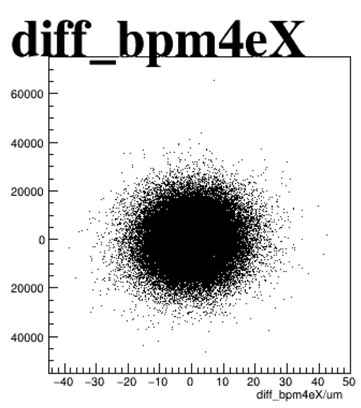

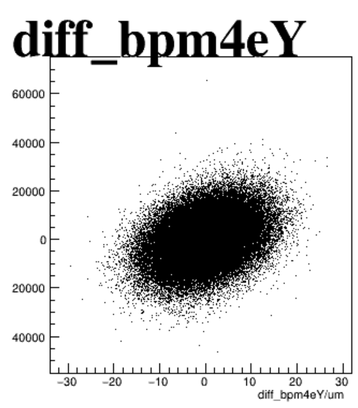

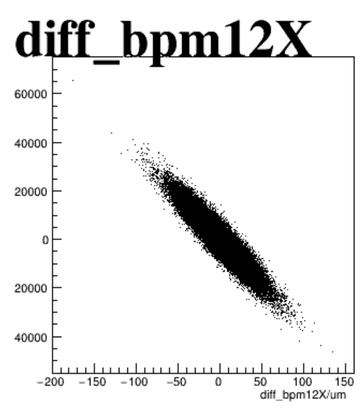

asym_atr2

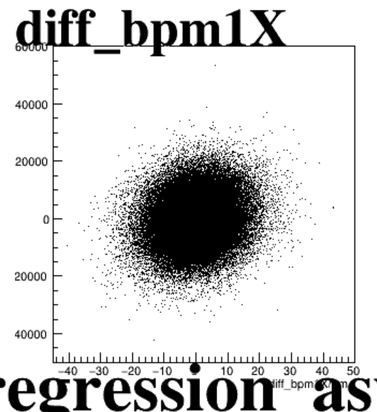

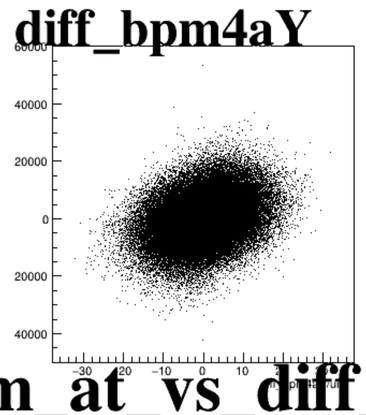

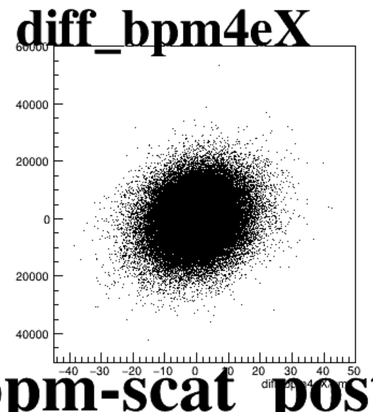

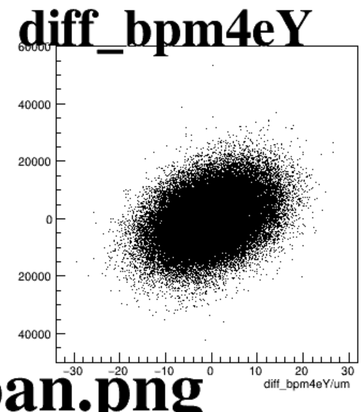

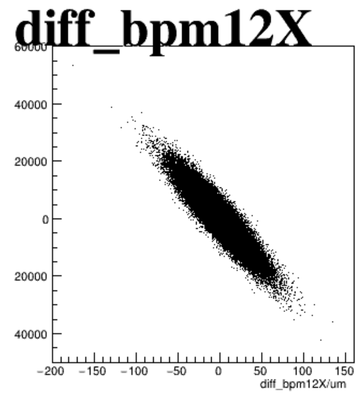

run6630_000_regression_asym_at_vs_diff_bpm-scat_postpan.png

reg_asym_atl1

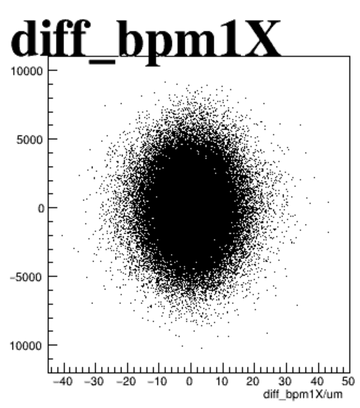

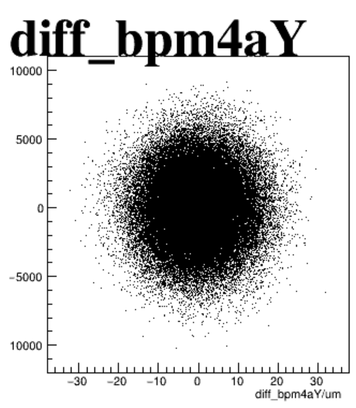

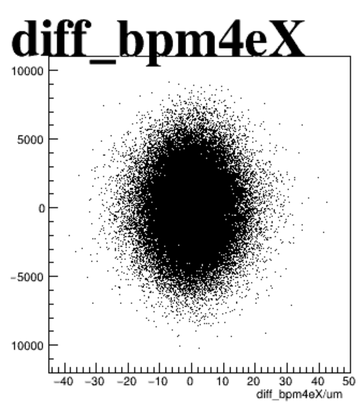

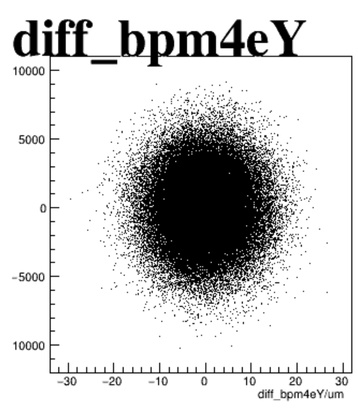

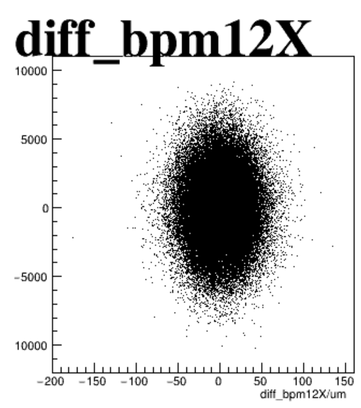

reg_asym_atr1

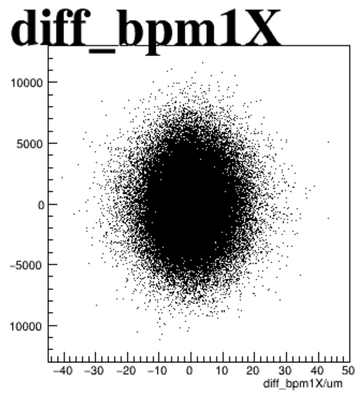

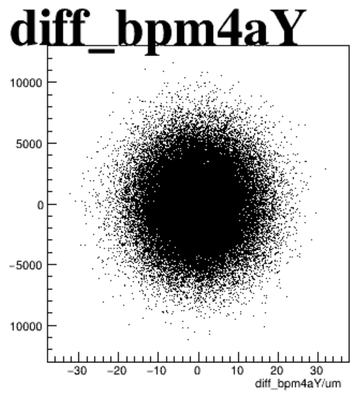

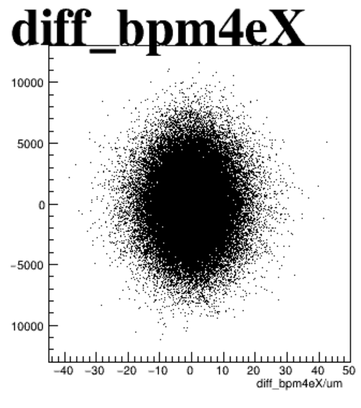

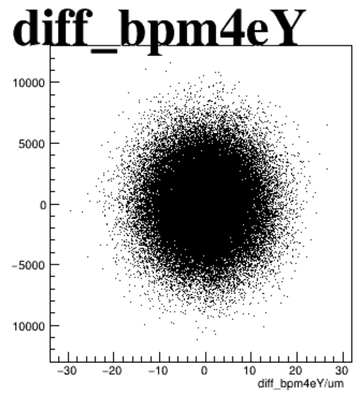

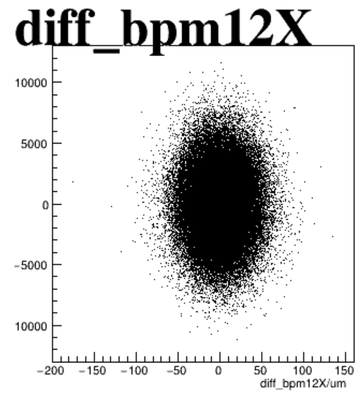

reg_asym_atl2

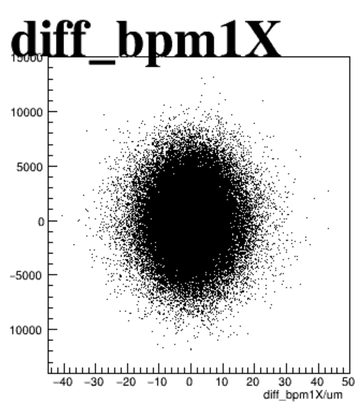

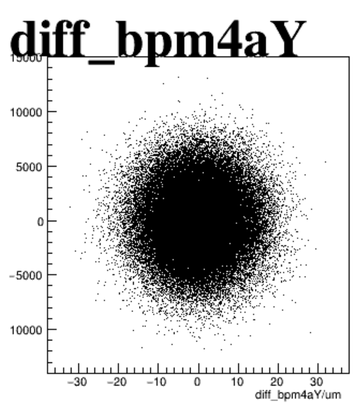

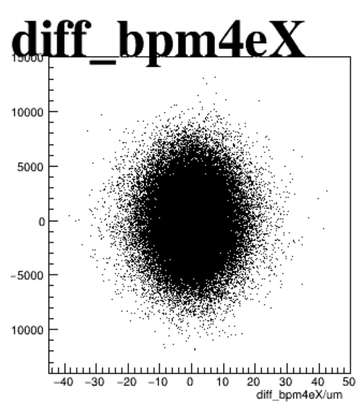

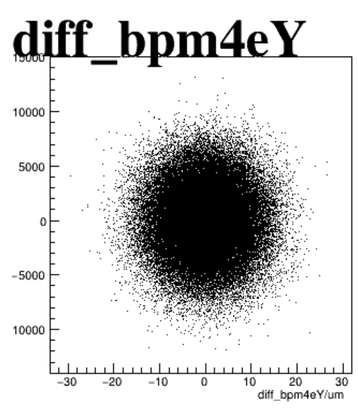

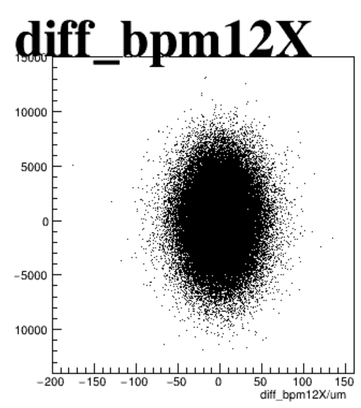

reg_asym_atr2

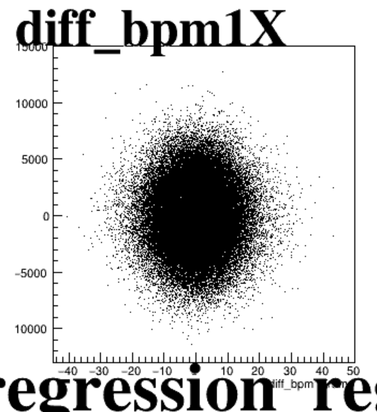

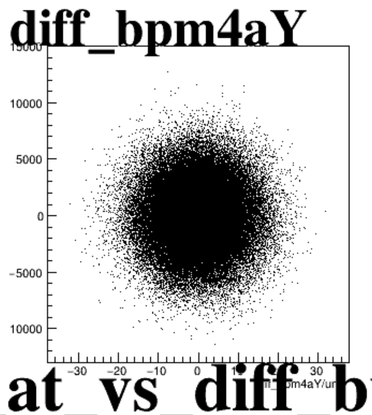

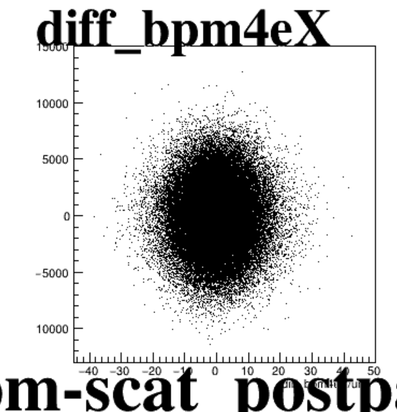

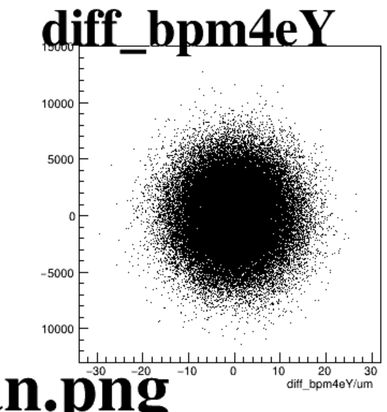

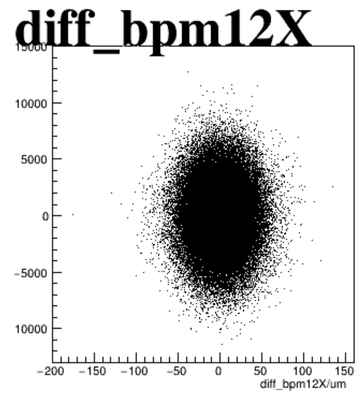

run6630_000_regression_reg_at_vs_diff_bpm-scat_postpan.png